Comparison of Kalman and interval approaches for the simultaneous localization and mapping of an underwater vehicle

J. Nicola and L. Jaulin

***Abstract*—In this paper we compare the use of a Kalman filter and a Robust State Observer for the localization and mapping of an underwater vehicle using range-only measurements between the vehicle and a set of beacons lying on the seafloor. As expected, we show that the Kalman filter performs great when we have a reasonably good prior information on the location of the vehicle and the beacons. Based on set-membership methods, the Robust State Observer demonstrates an outstanding capacity to provide consistent estimates (where the true solution is in the estimated confidence domain) in the presence of outliers at the cost of a very coarse precision. The source of this lack of precision will be discussed.**

***Index Terms*—SLAM, Kalman filter, interval analysis, robust estimation, set-membership estimation, underwater robotics.**

I. Introduction

Simultaneous Localization and Mapping [1], [2] is the problem of estimating the pose of a vehicle while building a map of its environment. The more precisely the pose is known, the more precise the map will be and reciprocally. In an underwater positioning context, where GPS is not available and SLAM can be seen as a solution for localization. It is possible to compute a crude estimation of the objects positions from the surface, and refine these positions on-the-go as an underwater vehicle navigates between them. It is even possible to avoid completely the prior survey phase, and to go directly for the online calibration, which results in important time savings. SLAM needs a perception of the environment which are based on cameras, sonars and any other sensors. In the context of this paper, the exteroceptive sensor which is used is an acoustic range-only sensor.

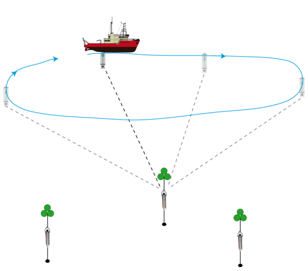

Fig. 1. Pre-survey from a surface vessel

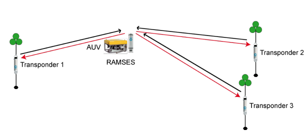

Fig. 2. Navigation of an AUV in the calibrated baseline

This type of state estimation problem is typically solved with a Kalman filter [3], as it is a well studied, well understood state estimator that has successfully been applied on a number of localization and SLAM related problems [4], [5], [6]. While this approach works remarkably well when a good initial estimate is available for the position of the mobile and the beacons, it is known to suffer from poor performances when the system is not well conditioned, when nonlinearities occur and no good initial estimate is known. In these situations, a Kalman filter can produce a poor estimate with a high confidence, and will reject good measurements, being unable to distinguish them from outliers, making it tricky to detect a fault. In this article, we will compare a Kalman filter approach with an other approach based on set-theory [7]. Set-theoretic approaches are interesting because they are probabilistic agnostic and some of them are applicable to nonlinear systems with robustness to outliers. [8] compared the use of a Kalman filter for the localization of a terrestrial vehicle with interval methods.

In this paper, we compare and combine set-membership and probabilistic approaches to solve the SLAM problem for an underwater vehicle. Underwater localization [9][10] mainly relies on the fact that the time of flight of the sound provides us the distance between the robot and some seamarks. And in this situation, set-membership methods have been shown to be very attractive [11][12].

The paper is organized as follows. Section II describes the modelisation of the system and its sensors, with the assumptions on the nature of uncertainties. In Section III we see how our problem can be cast in a probabilistic state estimation problem, and study the use of a Kalman filter to solve it. Section IV briefly recalls the principles behind interval-based state estimation with its theoretical advantages and drawbacks. Section V compares both methods on a real data set. Section VI discusses the results, and in particular the source for the lack of precision for the interval estimator. Section VII concludes the paper.

II. Modeling the problem

SLAM is a typical state estimation problem [13] that is described by the following state equations [14]:

$$\begin{cases} \mathbf{x}_{k+1} &= \mathbf{f}_k(\mathbf{x}_k) \\ \mathbf{y}_k &= \mathbf{g}_k(\mathbf{x}_k) \end{cases} \tag{1}$$

where k is the time, $\mathbf{x} = (\mathbf{x}_m, \mathbf{x}_{b_1}, \mathbf{x}_{b_2}, \ldots, \mathbf{x}_{b_N})$ is the state vector, containing the position $\mathbf{x}_m$ of the mobile and the beacons $\mathbf{x}_{b_i}$ and $\mathbf{y}$ is the observation vector. The function $\mathbf{f}$ in the first equation is the evolution function. It models the dynamic part of the problem. The function $\mathbf{g}$ is the observation function that models the exteroceptive measurements the vehicle makes on its environment.

A. Evolution equation

In this paper, we work in an underwater environment and we now describe the sensor we use for navigation and SLAM. For its proprioceptive sensors, the vehicle is equipped with a PHINS [15], a fiber optic gyroscope inertial navigation system made by iXBlue [16], a DVL and a pressure sensor. These sensors can be considered as proprioceptive since they are involved in the evolution equations. These proprioceptive sensors can be considered as reliable (*i.e.*, without ouliers) and accurate.

Fig. 3. A PHINS 6000 coupled with a DVL

Fig. 4. The RAMSES acoustic navigation system

The evolution equation of the mobile can be formulated as:

$$\mathbf{x}_{m_{k+1}} = \mathbf{x}_{m_k} + \mathbf{R}(\phi_k, \theta_k, \psi_k) \cdot \mathbf{u}_k + \boldsymbol{\alpha}_k \tag{2}$$

where $\mathbf{R}(\phi, \theta, \psi)$ is the Euler matrix of the vehicle depending on the Euler angle (ϕ, θ, ψ) given by the INS. The vector $\mathbf{u}$ is the speed of the vehicle in the robot frame, and $\boldsymbol{\alpha}$ some noise.

In a typical setup, the sources of uncertainties come from:

- Misalignment or imprecisely known lever arms between the sensors.
- Noise on the collected Euler angles and accelerations.
- Noise on the measured speed.

We consider that the vehicle that runs the experiment is perfectly characterized so that we know precisely the lever arms and the alignments between the sensors. Since the INS gives the attitude of the vehicle with a very high precision, as a first approximation we do not consider the contribution of these noises. The DVL measures the speed of the vehicle by measuring the Doppler shift of a high-frequency acoustic signal projected on the seafloor. Because these measurements are not highly reliable, we consider that they are the main source of uncertainties on the evolution equation of the mobile. Therefore, $\boldsymbol{\alpha}_k$ is modeled as a perturbation whose only contribution is considered to come from the integrated measured speed. Since the beacons are tied to the seafloor, the evolution equation of the i^{th} beacon is simply:

$$\mathbf{x}_{b_{i_{k+1}}} = \mathbf{x}_{b_{i_k}} \tag{3}$$

B. Observation equation

For its exteroceptive sensors the robot uses a classical pressure center which provides the depth of the robot. The vehicle is also equipped with a RAMSES [17], a synthetic baseline acoustic positioning device developed by iXBlue [16] that measures the range between the device and a beacon by measuring the times-of-flight of an acoustic signal sent to, and the acoustic signal answered by the beacon.

Therefore, the observation equation for the seamark observed at instant k is written as:

$$y_k = \sqrt{(x_m - x_{b_k})^2 + (y_m - y_{b_k})^2 + (z_m - z_{b_k})^2} + w_k \tag{4}$$

which simply is a distance equation between the mobile and the beacon, plus some noise w.

The sources of uncertainties in the range measurements come from :

- *Approximate knowledge on the celerity profile*. The celerity profile is a function that maps the depth in the water to the celerity of the sound at this depth. It is used to convert the time of flight of an acoustic signal to a range information between the source and the receiver. It depends on several factors such as the pressure, the temperature, the salinity of the water. Depending on the location and the depth of the emitter and the receiver, the celerity profile can also vary with time.
- *The environment*. No line of sight might be present between the emitter and the receiver, and multipath can be received, introducing outliers in the measurements.
- *Uncertainties on the sensor's internal functioning*. These uncertainties are characterized precisely in laboratory.

Since it is hard to quantify and propagate the uncertainties on the celerity profile and the environment, in this paper we assume that the perturbation on the measurement is additive. This is a gross simplification that works well for the orders of magnitude involved in our experiments. Moreover, due to multiple echos, interferences, unmapped obtacles, etc., outliers may occur.

Exteroceptive outliers is one of the main difficulty met in practice. It that has to be considered in order to build reliable underwater robots.

III. Solving with a Kalman Filter

Probabilistic state estimation is the classical approach for state-estimation in robotics [18], [13]. It relies on statistical techniques to integrate imperfect models with imperfect sensing. The most widely used approach for probabilistic state-estimation are the Bayes filters, that offers a methodology for estimating a probability distribution over the state, conditioned on all available data in a recursive manner. The two most widely used Bayesian filters are the Kalman filter and the Particle filter. In this paper, we will focus on Kalman filtering, commonly used in the industry.

A. Kalman filtering

The Kalman filter is the best studied approach to implementing a Bayes filter. It represents the knowledge we have about the estimated random variables at time k by their first two statistical moments: the mean $\boldsymbol{\mu}_k$ and the covariance matrix $\boldsymbol{\Gamma}_k$.

1) Prediction equation: The Kalman filter assumes that the evolution model is linear with additive, normally distributed, white noise expressed by the following equation:

$$\mathbf{x}_{k+1} = \mathbf{A}_k \cdot \mathbf{x}_k + \mathbf{B}_k \cdot \mathbf{u}_k + \boldsymbol{\alpha}_k. \tag{5}$$

In our model $\mathbf{A}_k$ is simply the identity matrix at every time k, $\mathbf{B}_k$ is the Euler rotation matrix defined above, and $\mathbf{u}_k$ is the integrated speed. The noise vector is denoted by $\boldsymbol{\alpha}_k$. Since this noise is considered to come from the integrated speed, its covariance matrix is approximated by:

$$\boldsymbol{\Gamma}_{\boldsymbol{\alpha}_k} = \mathbf{R}_k \cdot \boldsymbol{\Gamma}_{\boldsymbol{v}_k} \cdot \mathbf{R}_k^T \tag{6}$$

with $\boldsymbol{\Gamma}_{\boldsymbol{v}_k}$ the covariance matrix of the integrated speed expressed in the local frame of the vehicle at time k. Our model is suitable for the use of a Kalman filter, because not only is there no multiplicative noise involved, but the equation is linear with respect to the inputs and the state vector.

The Kalman filter prediction equations are thus

$$\begin{cases} \hat{\mathbf{x}}_{k+1} &= \hat{\mathbf{x}}_k + \mathbf{B}_k \cdot \mathbf{u}_k \\ \boldsymbol{\Gamma}_{k+1} &= \boldsymbol{\Gamma}_k + \boldsymbol{\Gamma}_{\boldsymbol{\alpha}_k} \end{cases} \tag{7}$$

When initializing the filter, $\hat{\mathbf{x}}_0$ must be chosen as close as possible to the real position of the vehicle and the beacons. The matrix $\boldsymbol{\Gamma}_0$ must be chosen to reflect the amount of uncertainty on this initial belief. For example, when no good prior information on the localization of a beacon is known, the covariance matrix associated with its position can be set diagonal with very large diagonal elements.

2) Update equation: For a Kalman filter to apply, the observation equations must be linear in the state vector variables, and subject to additive Gaussian noise. The additive Gaussian noise assumption, while widely used, is a crude simplification of the real noise that is applied to our observations. Indeed, some of those uncertainties, especially the ones on the celerity profile, have no reason to be modeled as Gaussian. The whiteness assumption is also not reasonable: if an object is present between the sensor and a beacon at time k, adding a bias to the measured time of flight, it is very likely that this bias will be present in a neighborhood of k. From Equation 4 it is also clear that the linearity assumption does not hold. There exists mainly two methods to apply a Kalman filter with nonlinear models:

- Extended Kalman Filter: this approach consists of linearizing the equations by Taylor series expansion around of the current estimated mean to be able to apply the Kalman filter update equations.
- Unscented Kalman Filter [19]: this approach propagates a finite set of sample points, called sigma points, around the mean through the nonlinear function, from which the posterior mean and covariance matrix of the estimate are computed. This flavor captures more accurately the true mean and covariance of the estimate.

However, even if the observation noise is really Gaussian, the probability density function of the estimate is very unlikely Gaussian due to the nonlinearities. Therefore, the two first statistical moments might not contain enough information to correctly represent the true estimated distribution.

3) Dealing with outliers: A criteria can be defined on the innovation of a specific observation to decide if we should accept or reject it. With $\tilde{\mathbf{y}}_k$ the innovation at time k, defined by the difference between the predicted and the actual observation and, $\mathbf{S}_k$ the covariance of the innovation, and a confidence threshold η, we consider the condition

$$\tilde{\mathbf{y}}_k \cdot \mathbf{S}_k^{-1} \cdot \tilde{\mathbf{y}}_k^T < \alpha(\eta). \tag{8}$$

If this condition is not satisfied, that is, if the observation is too distant from the predicted observation, the measurement $\mathbf{y}_k$ is rejected. The quantity $\alpha(\eta)$ gives the radius of the confidence ellipsoid given a confidence threshold η. This criteria is also found under the name of Mahalannobis distance in the literature. It works remarkably well when the estimate is "close" to the real solution. But when it is not the case, this criteria will eventually discard good observations, because the estimate has not converged to the real solution yet. This is especially the case when no good initialization is available for the filter. Empirical strategies must then be put in place to allow for some of these measurements to be integrated anyway. Note that the exitence of outliers is not rare in an underwater acoutic system due to multiple echos, interferences, etc.

IV. Solving with sets

Set-membership methods propose a non-stochastic approach to treat uncertainties, by making the assumption that the noises are unknown but bounded. The estimated variables are enclosed in sets. Different representations for sets are available: zonotopes [20], ellipsoids [21], [22], intervals [23], [24], subpavings [25], [26]. Such representations have several advantages:

- Since only the support of the density distribution function for the uncertainties are considered, they are compatible with an infinite number of distribution functions.
- For the case of interval and subpaving representations, no linearization is required since these representation can be propagated through any nonlinear function.
- For the case of intervals and subpavings, there exist a scheme for dealing with outliers based on the q-relaxed intersection [27].

Since in this paper we face the problem of unknown noises and nonlinearities, we retained the interval and subpaving representations. [23] presents a state-estimator based on interval analysis which alternates prediction and correction steps the same way as a Kalman filter. [28] compares this approach with an approach based on constraint propagation. Both methods should be combined and made robust with respect to outliers as proposed in [7], which is the chosen approach for this paper.

A. Principle

It is assumed that the initial state $\mathbf{x}_0$ belongs to a known set $\mathbb{X}_0$, and that $\mathbf{y}(k)$ belongs to some sets $\mathbb{Y}(k)$ (which are intervals). The set $\mathbb{X}(k)$ containing all the feasible state vectors at time k can be computed recursively [29] by the relation

$$\mathbb{X}(k+1) = \mathbf{f}_k\left(\mathbb{X}(k) \cap \mathbf{g}^{-1}(\mathbb{Y}(k))\right).$$

W can also consider the following equation

$$\mathbb{X}(k+1) = \mathbf{f}_k(\mathbb{X}_k) \cap \bigcap_{i \in \{0,\dots,\ell\}} \mathbf{f}_k^i \circ \mathbf{g}_k^{-1}(\mathbb{Y}(k-i)) \quad (9)$$

with

$$\mathbf{f}_k^i = \mathbf{f}_k \circ \mathbf{f}_{k-1} \circ \cdots \circ \mathbf{f}_{k-i}. \quad (10)$$

This equation defines the set of for all state vectors that are consistent with all data inside a time window of length ℓ.

B. Dealing with outliers

It happens that some $\mathbf{y}(k)$, the actual value of the observed quantity at time k, do not belong to their corresponding set $\mathbb{Y}(k)$. $\mathbf{y}(k)$ is said to be an inlier if $\mathbf{y}(k) \in \mathbb{Y}_k$, and an outlier otherwise. With the assumption that there are at most q outliers among the last l observations, the set given by the$q$-relaxed intersection $\overset{q}{\cap}_{i\in\{0,\dots,l\}} \mathbf{f}_k^i \circ \mathbf{g}_k^{-1}(\mathbb{Y}(k-i))$ is guaranteed to contain $\mathbf{x}(k)$. The q-relaxed intersection $\overset{q}{\cap}$ is a set operation that computes the classical intersection of m sets except q of them.

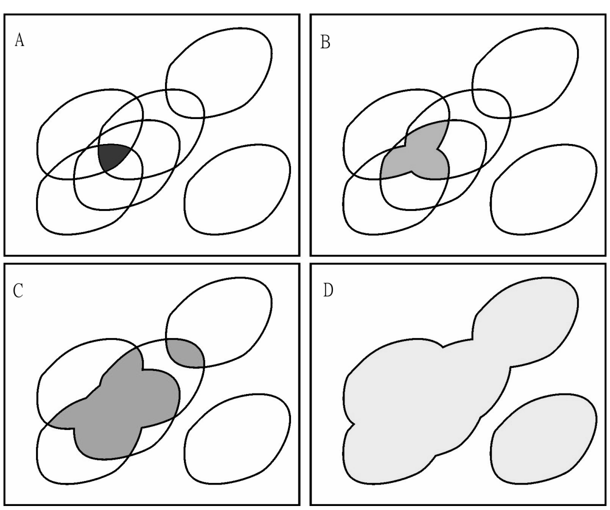

Fig. 5. Q-relaxed intersection of 6 sets with respectively A) $q = 2$, B) $q = 3$, C) $q = 4$, D) $q = 5$.

Computing the q-relaxed intersection of n intervals is solved in $O(n.log(n))$. However, when q is not fixed, the complexity of computing the q-relaxed intersection grows exponentially with the dimension of the boxes. Algorithms that compute an overestimation of the true q-intersection have to be used. For a complete review of the q-intersection algorithms the reader is referred to [27], [30].

C. Robust State Estimator

Using the tools defined in Sections IV-A and IV-B, we propose the Robust State Estimator (RSO) [7]

$$\text{RSO:} \begin{cases} \mathbb{X}(k) = & \mathbf{f}_k^0(\mathbb{X}_0) \text{ if } k < m \ (initialization) \\ \mathbb{X}(k) = & \mathbf{f}_k^{k-m}(\mathbb{X}(k-m)) \cap \\ & \bigcap_{i\in\{0,\dots,\ell\}}^{\{q\}} \mathbf{f}_k^i \circ \mathbf{g}_k^{-1}(\mathbb{Y}(k-i)) \text{ if } k \geq m \end{cases} \quad (11)$$

where q is the number of outliers that are allowed inside the time window of length ℓ. This estimator is proved to be robust with respect to outliers.

V. Comparison

In this section, we compare the two approaches on a dataset acquired near La Ciotat, France in February 2014. A ship (the *vehicle*) is equipped with a PHINS [15], a RAMSES [17], a DVL, a GPS and an acoustic modem to measure distances between existing beacons. It performs a survey of a zone where 4 acoustic beacons lie on the seafloor. The position of these 4 seamarks are precisely known. The trajectory of the ship and the position of the seamarks are depicted in Figure 6. This trajectory is obtained by a fusion of the GPS with the INS sensors. It can be considered as our ground truth. The vehicle (the ship) plays here the role of an underwater robot. Since it is always at the surface, a pressure sensor is not needed. We assume here that the depth is measured as zero with an error of $\pm$1meter.

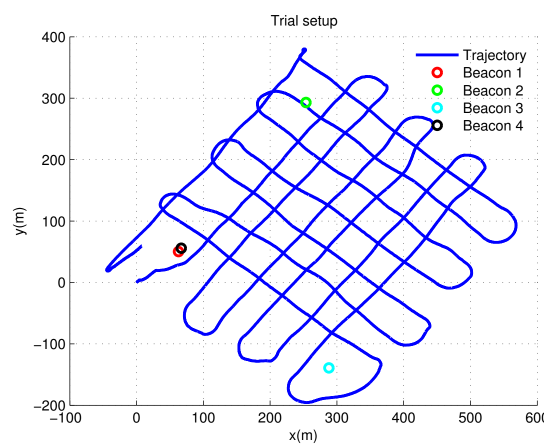

Fig. 6. Illustration of the experiment used for the comparison

A. Methodology

We will first run a test-case where the vehicle position is assumed to be perfectly known since the start of the mission, and the beacons positions are known up to a bias in the order of magnitude of 30 meters in the X/Y plane. We will then run a test-case where the vehicule position is still assumed to be perfectly known, but the seamarks X/Y coordinates are supposedly totally unknown. In this case, the Kalman filter for the seamarks is initialized on the initial position of the vehicle with a very large covariance matrix. In both scenarios, the altitude of the beacons is known with a precision of about one meter. We will compare the two approaches for the estimation of the vehicle's and the seamark's positions.

Consistency. An estimation is said to be *consistent* if the true value of the estimated quantity is contained in the confidence domain provided by the filter. For the Kalman filter, we will say that an estimated position is consistent if the true position is inside its 99% confidence ellipse. For the RSO, the estimation is consistent if it is contained in its subpaving. We will compare the rate of consistency for both filters during all the mission.

Error. We define the estimation error as the Euclidian distance that separates it from the true value. For the Kalman filter, it will be the distance between its mean and the true position, for the RSO it will be the distance between the center of mass of the subpaving and the true position.

B. SLAM with some initial knowledge

Figure 7 displays the confidence domains for the error on the x (Easting) and y (Northing) positions of the vehicle in the local frame for the Kalman filter and the RSO. The Kalman filter gives an estimate with an decimetric error, while the RSO gives a decametric errors. Both approaches contain the real position during all the mission.

Regarding the estimated positions of the beacons shown in Figure 8, the Kalman filter converges in less than 10 minutes to a decimetric precision, while the RSO's precision quickly reaches a decametric precision and doesn't improve after that. Both approaches provide consistent estimations: the corresponding sets contain the true positions of the beacons during all the mission.

Vehicle's precision	UKF	RSO
Max. Error - m	1.15	71.48
Final Error - m	0.469	9.57
Consistency - %	100	100

TABLE I
PRECISION FOR THE VEHICLE'S LOCALIZATION WHEN A SMALL BIAS IS ADDED TO THE BEACON'S POSITIONS

	Beacons precision	UKF	RSO
Beacon 1	Final Error - m	0.246	10.99
	Initial bias - m	28.7	
	Consistency - %	100	100
Beacon 2	Final Error - m	0.180	7.45
	Initial bias - m	22.8	
	Consistency - %	100	100
Beacon 3	Final Error - m	0.221	7.56
	Initial bias - m	35.1	
	Consistency - %	100	100
Beacon 4	Final Error - m	0.657	9.05
	Initial bias - m	30.1	
	Consistency - %	40.63	100

TABLE II
PRECISION FOR THE BEACONS LOCALIZATION WHEN A SMALL BIAS IS ADDED TO THEIR INITIAL POSITIONS

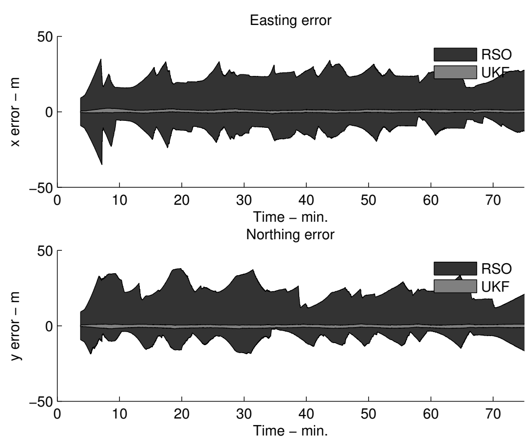

Fig. 7. Confidence for the Easting and the Northing of the trajectory when the base is biased

C. SLAM without initial knowledge

Figure 9 shows that the confidence on the error of the vehicle's position is higher than for the previous scenario. However, both filters are consistent during the whole mission: their 99% confidence domains for the vehicle's positions contain the true position. Regarding the estimation of the beacon's positions, the Kalman filter is able to locate the second beacon with a final error of about 4 meters, while it converges to wrong positions for the other beacons, whose 99% confidence domains do not contain the true positions. The RSO on the other hand, is able to locate the beacons with a final error of about 10 meters for all the beacons, and the true beacon's positions are contained in its estimate.

VI. DISCUSSION ON THE PESSIMISM OF THE RSO

Section V has shown that the RSO's precision, despite having a 100% consistency, is quite unsatisfying. One might argue that its high consistency comes from its high level of pessimism. In this section, we describe two factors that have been identified as a unnecessary source of pessimism.

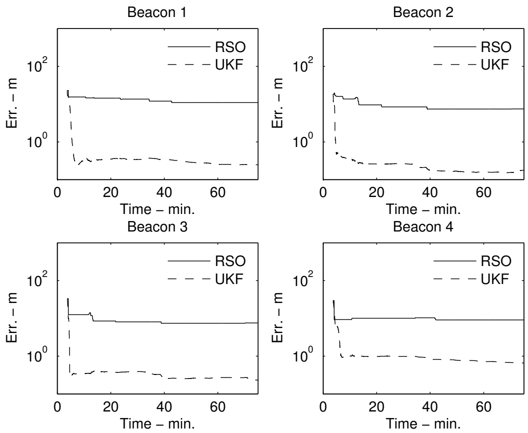

Fig. 8. Estimation errors of the beacon's positions when their initial positions are biased

Vehicle's precision	UKF	RSO
Max. Error - m	4.76	71.48
Final Error - m	3.73	19.0
Consistency - %	83.9	100

TABLE III
PRECISION FOR THE VEHICLE'S LOCALIZATION WHEN THE BEACON'S POSITIONS ARE UNKNOWN

	Beacons precision	UKF	RSO
Beacon 1	Final Error - m	458.2	6.40
	Initial bias - m	319.8	
	Consistency - %	11.6	100
Beacon 2	Final Error - m	4.29	16.85
	Initial bias - m	80.4	
	Consistency - %	68.9	100
Beacon 3	Final Error - m	332.7	17.83
	Initial bias - m	87.1	
	Consistency - %	24.6	100
Beacon 4	Final Error - m	48.7	13.52
	Initial bias - m	387.6	
	Consistency - %	17.5	100

TABLE IV
PRECISION FOR THE BEACONS LOCALIZATION WHEN THE INITIAL LOCATION OF THE VEHICLE IS UNKNOWN

A. Wrapping effect

Definition 1. A transformation T is said to be box-conservative if the image of an axis-aligned box through T is also an axis-aligned box.

Remark 2. The evolution model for the vehicle involves a rotation that maps the speed measured in the local vehicle's frame to the global frame. A rotation is generally not box-conservative, and this rotation adds pessimism known as wrapping-effect [31].

Since the evolution model is linear, intervals are not the best representation for sets. For this kind of models, other methods such as zonotopes or ellipsoids are a more attractive representation. To reduce the wrapping induced by the rotation, a combination of linear and interval methods could be used.

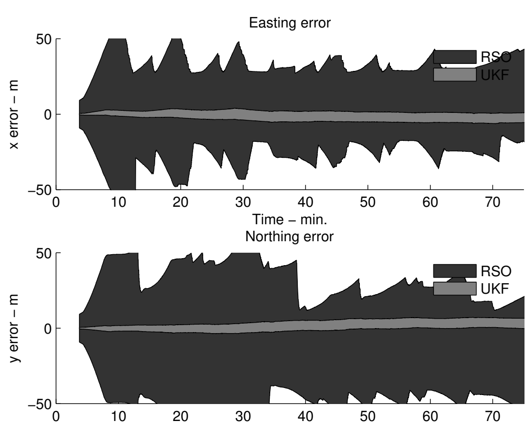

Fig. 9. Confidence the Easting and the Northing of the vehicle when the base is unknown

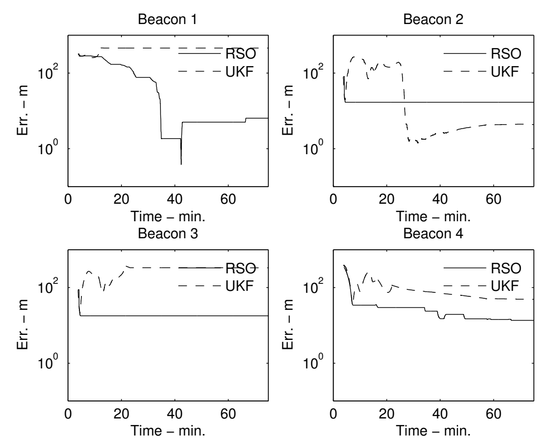

Fig. 10. Precision for the beacons when the base is unknown

B. Non-compensation of noises

Assume the robot moves in a fixed direction. We have $\forall k, \mathbf{R}_k = \mathbf{R}, \mathbf{\Gamma}_{\alpha_k} = \mathbf{\Gamma}_\alpha$. At the beginning the robot knows its exact position, so $\mathbf{\Gamma}_0 = 0$. If the robot does not make any observation, we have the following properties.

Proposition 3. *Without exteroceptive measurements, the precision given by a Kalman filter for the position of the system described in Equation 2 grows as a square-root of the time.*

Proof: Following Equation 7, we have

$$\begin{cases} \mathbf{\Gamma}_1 & = \mathbf{\Gamma}_\alpha \\ \mathbf{\Gamma}_2 & = \mathbf{\Gamma}_1 + \mathbf{\Gamma}_\alpha = 2 \cdot \mathbf{\Gamma}_\alpha \\ \vdots & \\ \mathbf{\Gamma}_k & = k \cdot \mathbf{\Gamma}_\alpha \end{cases}. \tag{12}$$

Given a fixed time-step dt between instant k and instant $k+1$, the elapsed time is $t = k \cdot dt$, and we have

$$\mathbf{\Gamma}_k = \frac{t}{dt} \cdot \mathbf{\Gamma}_\alpha. \tag{13}$$

A confidence domain with confidence η for a random variable x following a normal distribution with mean μ and variance σ^2 is described by the following inequality

$$(x-\mu)^2 \leq \alpha^2(\eta) \cdot \sigma^2 \tag{14}$$

with $\alpha(\eta)$ a function that gives the confidence threshold α for a confidence η. Consequently, for any of the mobile's position component x_i, we have

$$\sqrt{\frac{(x_i - \hat{x}_i)^2}{\alpha^2(\eta) \cdot \Gamma_{\alpha_{ii}}} \cdot dt} \leq \sqrt{t} \tag{15}$$

which concludes the proof. ■

Proposition 4. *Without exteroceptive measurements, the precision given by the RSO for the position of the system described in Equation 2 grows linearly with time.*

Proof: The perturbation on the integrated speed in 1 is supposed to belong to some interval $[\mathbf{w}_\alpha]$.

From we have

$$\begin{cases} [\boldsymbol{x}_{m_1}] & = \boldsymbol{x}_{m_0} + \mathbf{R} \cdot \mathbf{u} + [\mathbf{w}_\alpha] \\ [\boldsymbol{x}_{m_2}] & = [\boldsymbol{x}_{m_1}] = \boldsymbol{x}_{m_0} + 2 \cdot \mathbf{R} \cdot \mathbf{u} + 2 \cdot [\mathbf{w}_\alpha] \\ \vdots & \\ [\boldsymbol{x}_{m_2}] & = \boldsymbol{x}_{m_0} + k \cdot \mathbf{R} \cdot \mathbf{u} + k \cdot [\mathbf{w}_\alpha] \end{cases} \tag{16}$$

Given a fixed time-step dt between instant k and instant $k+1$, the elapsed time is $t = k \cdot dt$, and with $w([x])$ the width of an interval $[x]$, we have

$$w\left(\left[x_{m_{k_i}}\right]\right) = \frac{t}{dt} \cdot w\left([w_{\alpha_i}]\right)$$

which concludes the proof. ■

Propositions 3 and 4 shows that the Kalman filter is much more precise when integrating the proprioceptive measurements than its interval counterpart. By taking into account that the proprioceptive noises are Gaussian, it is able to provide a precision that grows as a square root of the time, whereas the RSO provides an estimate whose precision grows linearly with time.

VII. Conclusion

In this paper, we compared the use of a Kalman filter against an interval filter for the SLAM problem of a vehicle (here a ship) on a real data set. As expected, the Kalman filter gives estimates that are of high precision when we have a reasonable prior knowledge on the beacons positions, and might converge towards wrong solutions when no such knowledge is available. The RSO, on the other hand, is consistent during all the mission with or without good prior knowledge, but its precision is quite poor. To improve the precision of the Kalman filter, we could use an approach similar to [32], where the initial state is first estimated with an interval method, and then a Kalman filter is initialized from this estimate. An other approach would be to overcome the sources of pessimism described in Section VI. Since the evolution model is linear, the wrapping effect could be reduced by combining an interval approach with a linear approach such as ellipsoidal methods [22], [29], [33]. An other way of drastically reducing the pessimism of the RSO would be to make it able to integrate the uncertainties as a square-root of time, which would make the propagation-retropropagation described in Equation 10 much more precise.

References

[1] R. C. Smith and P. Cheeseman, "On the representation and estimation of spatial uncertainly," *Int. J. Rob. Res.*, vol. 5, no. 4, pp. 56–68, Dec. 1986.

[2] J. Leonard and H. Durrant-Whyte, "Simultaneous map building and localization for an autonomous mobile robot," in *Proceedings of the IEEE/RSJ International Conference on Intelligent Robots and Systems, IROS 1991, Osaka, Japan, November 3-5, 1991*, 1991, pp. 1442–1447.

[3] R. E. Kalman, "A new approach to linear filtering and prediction problems," *Transactions of the ASME–Journal of Basic Engineering*, vol. 82, no. Series D, pp. 35–45, 1960.

[4] G. A. Kantor and S. Singh, "Preliminary results in range-only localization and mapping," in *Proceedings of the IEEE Conference on Robotics and Automation (ICRA '02)*, vol. 2, May 2002, pp. 1818 – 1823.

[5] E. Olson, J. Leonard, and S. Teller, "Robust range-only beacon localization," *Oceanic Engineering, IEEE Journal of*, vol. 31, no. 4, pp. 949–958, 2006.

[6] J. J. Leonard and H. F. Durrant-Whyte, "Mobile robot localization by tracking geometric beacons," *"IEEE Transactions on Robotics and Automation"*, vol. 7, no. 3, pp. 376–382, 1991.

[7] L. Jaulin, "Set-membership localization with probabilistic errors," *Robotics and Autonomous Systems*, vol. 59, no. 6, pp. 489–495, 2011.

[8] A. Gning and P. Bonnifait, "Dynamic vehicle localization using constraints propagation techniques on intervals A comparison with kalman filtering," in *Proceedings of the 2005 IEEE International Conference on Robotics and Automation, ICRA 2005, April 18-22, 2005, Barcelona, Spain*, 2005, pp. 4144–4149.

[9] B. Zerr, G. Mailfert, A. Bertholom, and H. Ayreault, "Sidescan sonar image processing for auv navigation," in *Oceans 2005-Europe*, vol. 1. IEEE, 2005, pp. 124–130.

[10] V. Creuze, "Robots marins et sous-marins ; perception, modélisation, commande," *Techniques de l'ingénieur*, 2014.

[11] A. Caiti, A. Garulli, F. Livide, and D. Prattichizzo, "Localization of autonomous underwater vehicles by floating acoustic buoys: a set-membership approach," *IEEE Journal of Oceanic Engineering*, vol. 30, no. 1, pp. 140–152, 2005.

[12] ——, "Set-membership acoustic tracking of autonomous underwater vehicles," *Acta Acustica united with Acustica*, vol. 5, no. 88, pp. 648–652, 2002.

[13] L. Jaulin, *Automation for Robotics*. ISTE editions, 2015.

[14] ——, *Mobile Robotics*. ISTE editions, 2015.

[15] "PHINS product page," https://www.ixblue.com/products/phins, accessed: 2015-12-07.

[16] "iXBlue website," http://ixblue.com, accessed: 2015-12-07.

[17] "RAMSES product page," https://www.ixblue.com/products/ramses, accessed: 2015-12-07.

[18] S. Thrun, W. Bugard, and D. Fox, *Probabilistic Robotics*. Cambridge, M.A.: MIT Press, 2005.

[19] S. J. Julier and J. K. Uhlmann, "A new extension of the kalman filter to nonlinear systems," 1997, pp. 182–193.

[20] M. Maiga, N. Ramdani, L. Travé-Massuyès, and C. Combastel, "A csp versus a zonotope-based method for solving guard set intersection in nonlinear hybrid reachability," *Mathematics in Computer Science*, vol. 8, no. 3-4, pp. 407–423, 2014.

[21] B. T. Polyak, S. A. Nazin, C. Durieu, and E. Walter, "Ellipsoidal parameter or state estimation under model uncertainty," *Automatica*, vol. 40, no. 7, pp. 1171 – 1179, 2004.

[22] F. Chernousko, "Ellipsoidal state estimation for dynamical systems," *Nonlinear Analysis: Theory, Methods & Applications*, vol. 63, no. 5-7, pp. 872 – 879, 2005.

[23] M. Kieffer, L. Jaulin, E. Walter, and D. Meizel, "Guaranteed mobile robot tracking using interval analysis," in *Proceedings of the MISC'99 Workshop on Applications of Interval Analysis to Systems and Control*, Girona, Spain, 1999, pp. 347–359.

[24] O. Lévêque, L. Jaulin, D. Meizel, and E. Walter, "Vehicule localization from inaccurate telemetric data: a set inversion approach," in *Proceedings of 5th IFAC Symposium on Robot Control SY.RO.CO.'97*, vol. 1, Nantes, France, 1997, pp. 179–186.

[25] V. Drevelle, L. Jaulin, and B. Zerr, "Guaranteed characterization of the explored space of a mobile robot by using subpavings," in *Proc. Symp. Nonlinear Control Systems (NOLCOS'13)*, Toulouse, 2013.

[26] L. Jaulin, "Range-only SLAM with occupancy maps; A set-membership approach," *IEEE Transaction on Robotics*, vol. 27, no. 5, pp. 1004–1010, 2011.

[27] C. Carbonnel, G. Trombettoni, P. Vismara, and G. Chabert, "Q-intersection algorithms for constraint-based robust parameter estimation," C. o. A. I. Proc. of AAAI, Ed. AAAI Press, Québec City, Canada, 2014, pp. 2630–2636.

[28] B. Vincke and A. Lambert, "Experimental comparison of bounded-error state estimation and constraints propagation," in *IEEE International Conference on Robotics and Automation, ICRA 2011, Shanghai, China, 9-13 May 2011*, 2011, pp. 4724–4729.

[29] D. P. Bertsekas and I. B. Rhodes, "Recursive state estimation for a set-membership description of uncertainty," *"IEEE Transactions on Automatic Control"*, vol. 16, no. 2, pp. 117–128, 1971.

[30] L. Jaulin and E. Walter, "Guaranteed robust nonlinear minimax estimation," *IEEE Transaction on Automatic Control*, vol. 47, no. 11, pp. 1857–1864, 2002.

[31] N. S. Nedialkov and K. R. Jackson, "A new perspective on the wrapping effect in interval methods for initial value problems for ordinary differential equations," in *in: Perspectives on Enclosure Methods*. Springer-Verlag, 1999, pp. 219–264.

[32] D. Bouvet and G. Garcia, "Guaranteed 3-d mobile robot localization using an odometer, an automatic theodolite and indistinguishable landmarks," in *Robotics and Automation, 2001. Proceedings 2001 ICRA. IEEE International Conference on*, vol. 4, 2001, pp. 3612–3617 vol.4.

[33] C. Durieu, B. Polyak, and E. Walter, "Ellipsoidal state outer-bounding for MIMO systems via analytical techniques," in *Proceedings of the IMACS—IEEE–SMC CESA'96 Symposium on Modelling and Simulation*, vol. 2, Lille, France, 1996, pp. 843–848.